Journal of Chromatography B 1080 (2018) 42–49

Contents lists available at ScienceDirect

Journal of Chromatography B

journal homepage: www.elsevier.com/locate/jchromb

Supercritical fluid chromatography-photodiode array detection-electrospray ionization mass spectrometry as a framework for impurity fate mapping in the development and manufacture of drug substances

Gregory F. Pirrone[1], Rose M. Mathew[1], Alexey A. Makarov, Frank Bernardoni, Artis Klapars, Robert Hartman, John Limanto, Erik L. Regalado*

Process Research and Development, MRL, Merck & Co., Inc., Rahway, NJ 07065, USA

ARTICLE INFO

Keywords:
Supercritical fluid chromatography-photodiode array detection-electrospray ionization mass spectrometry
Fate and purge, impurity fate mapping
Spike and purge testing, method development
Pharmaceutical analysis

ABSTRACT

Impurity fate and purge studies are critical in order to establish an effective impurity control strategy for approval of the commercial filing application of new medicines. Reversed phase liquid chromatography-diode array-mass spectrometry (RPLC-DAD-MS) has traditionally been the preferred tool for impurity fate mapping. However, separation of some reaction mixtures by LC can be very problematic requiring combination LC-UV for area % analysis and a different LC-MS method for peak identification. In addition, some synthetic intermediates might be chemically susceptible to the aqueous conditions used in RPLC separations. In this study, the use of supercritical fluid chromatography-photodiode array-electrospray ionization mass spectrometry (SFC-PDA-ESIMS) for fate and purge of two specified impurities in the 1-uridine starting material from the synthesis of a bis-piv 2′keto-uridine, an intermediate in the synthesis of uprifosbuvir, a treatment under investigation for chronic hepatitis C infection. Readily available SFC instrumentation with a Chiralpak IC column (4.6 × 150 mm, 3 μm) and ethanol: carbon dioxide based mobile phase eluent enabled the separation of closely related components from complex reaction mixtures where RLPC failed to deliver optimal chromatographic performance. These results illustrate how SFC combined with PDA and ESI-MS detection can become a powerful tool for direct impurity fate mapping across multiple reaction steps.

1. Introduction

The characterization and control of impurities formed within a drug substance manufacturing process is vitally important and must be thoroughly understood prior to the filing of a commercial synthetic route [1–4]. Each impurity can be effectively controlled by investigating its formation, downstream fate, and the point in the process where it is removed or purged. A common method known as “spike and purge testing,” “fate and purge” or “impurity fate mapping” is applied to monitor the purging capability of a robust synthetic route and to track the fate of the impurities through the manufacturing process [4–6].

It is important to point out that although ICHQ11 requires an overall understanding of the formation, fate, and purge of impurities; there are no specific regulatory requirements for demonstrating successful impurity fate and purge analysis with respect to identity, mass balance and/or percent recovery of spiked impurities and their downstream analogues. Nevertheless, preliminary identification, successful peak tracking, and an acceptable mass balance recovery should be a fundamental requirement of any fate and purge experiment based on general scientific principles.

Ultimately, mapping these impurities and their derivatives through multiple synthetic steps requires laborious and sometimes challenging chromatographic method development and optimization [6–9]. Initially, these methods are designed to chromatographically resolve the starting materials, process solvents, and reaction by-products from the desired product in each synthetic step. However, the level of analytical complexity increases significantly when specific impurities are deliberately spiked into the reaction at high levels as some impurities may participate in the reaction and lead to the formation of new derivative species that can be closely related to the desired product and the initial process impurities.

Modern LC column technologies combined with state-of-the-art instrumentation and detection offer powerful analytical tools for the

* Corresponding author.
E-mail address: erik.regalado@merck.com (E.L. Regalado).
[1] These authors contributed equally to this work.

https://doi.org/10.1016/j.jchromb.2018.02.006
Received 20 December 2017; Received in revised form 4 February 2018; Accepted 6 February 2018
Available online 08 February 2018
1570-0232/

separation and analysis of complex mixtures [10–12]. Nevertheless, some separations remain very challenging, most notably complex mixtures of closely related species where conventional RPLC approaches simply do not work or fail to deliver optimal results [13–16]. RPLC with Photo-Diode-Array (PDA) detection is the preferred technology used for batch release testing including LC area% (LCAP) and LC weight% (LCWP) analysis of intermediates and final Active Pharmaceutical Ingredients (API) [17,18]. These UV-based methods are also employed for the fate-and-purge studies. However, most of the preferred mobile phase additives used for improving chromatographic selectivity and UV detection during RPLC separations (*e.g.* phosphoric acid, perchloric acid with sodium perchlorate, potassium hexafluorophosphate, borate, citrate, *etc.*) [19] are not volatile and can damage mass spectrometry instrumentation, thereby requiring the development of another complementary LC-UV-MS method for the identification of byproducts from the impurity-spiking-experiments. Thus, the application of MS-compatible chromatographic methods for the fate and purge work required for commercial filing application would be beneficial.

Supercritical fluid chromatography (SFC) is a robust and well-established technique in the pharmaceutical industry for the separation and purification of enantiomers [20–25], and it is also quickly becoming a powerful tool for achiral separations [13,14,16,26–28]. Recent improvements in SFC-PDA sensitivity [29–31] and hyphenation of SFC with a diverse set of detectors including mass spectrometry [32–36], evaporative light scattering and charged aerosol detection [37–40] combined with improvements in column and stationary phase technologies [41–43] have expanded the use of SFC to new applications across multiple scientific disciplines in both academic and industry settings [44–48]. In addition, non-MS compatible additives are not typically used or needed to improve selectivity and peak resolution in SFC [49,50], thereby eliminating the necessity of developing different methods for area% and peak identity verification by MS as in "traditional" RPLC-based workflows. In this study, the use of SFC-PDA-MS detection for direct impurity fate and purge mapping is described. We illustrate the power and simplicity of this approach in cases where RPLC would not be optimal.

2. Experimental

2.1. Instrumentation

Chiral SFC experiments were performed on a Waters Acquity UPC^2 (Waters Corp., Milford, MA, USA) systems equipped with a fluid delivery module (a liquid CO_2 pump and a modifier pump), a sampler manager – FL autosampler, two auxiliary column managers allowing six installed columns, a photodiode array detector, an SQD mass detector and MassLynx® software, version 4.1. Reversed phase high performance liquid chromatography (RPLC) experiments were performed on an Agilent 1200 (Agilent Technologies, Santa Clara, CA). The Agilent 1200 stack comprised of a G1379B degasser, a G1312B binary pump, a G1367C HiP-ALS SL autosampler, a G1315C diode-array detector and a 6140 single quadrapole mass detector. The system was controlled using Chemstation software.

2.2. Chemicals and reagents

Methanol and acetonitrile (HPLC Grade) were purchased from Fisher Scientific (Fair Lawn, NJ, USA). 2′keto-uridine intermediate and process impurities were synthesized in-house (Merck & Co., Inc., MRL, Rahway, NJ, USA). Ammonium Formate (NH_4HCO_2), uracil, 5-Br-uracil, ribosyl dimer, cytidine and uridine were all purchased from Sigma-Aldrich (St. Louis, MO, USA). Ultrapure water was obtained from a Milli-Q Gradient A10 from Millipore (Bedford, MA, USA). Bone dry-grade CO_2 was obtained from Air Gas (New Hampshire, USA).

2.3. Cytidine and ribosyl uridine fate and purge experiments

Pivaloyl chloride was added slowly to a solution of uridine and 1 wt % cytidine or 2 wt% ribosyl uridine impurities in pyridine. After some reaction workup the organic phase was concentrated and then distilled with toluene to provide a solution of pivaloyalated uridine and spiked impurities in toluene (end of pyvaloylation reaction: EOR-P). The solution of pivaloyalated products was then rediluted with toluene and treated with boron trifluoride diethyl etherate (BF_3). After heating for > 12 h, the reaction mixture was cooled and washed multiple times to give a solution of bis-piv uridine 2′OH (desired isomer) and pivaloyalated spiked impurities in toluene (end of isomerization reaction: EOR-I). The stream from isomerization step was treated with a mixture of chemical oxidants over 12 h at low temperature. The reaction was quenched, and the product bis-piv 2′ketouridine was isolated by direct crystallization from the reaction mixture.

2.4. RPLC-UV-MS conditions

RPLC-UV-MS separation was performed on a 3.0 mm × 100 mm, 3 µm Ascentis Express C18 column (Sigma-Aldrich, St. Louis, MO, USA) by gradient elution at a flow rate of 0.75 mL/min. The LC eluents were 2 mM NH_4HCO_2, pH 3.5 (aq) for solvent A and 90:10 CH_3CN: 2 mM NH_4HCO_2, pH 3.5 (aq) for solvent B. The mobile phase was programmed as follows: linear gradient from 5 to 95% B in 28 min, hold at 95% B for two minutes and finishing with a 5 min post-run equilibration. The column was maintained at a temperature of 45 °C. The mass spectrometer settings were as follows: both positive and negative ion spectra were acquired using API-ES with a capillary voltage of 3.0 kV, fragmentor voltage of 70 V, drying gas flow of 12.0 L/min, drying gas temperature of 350 °C. Full-scan mass spectra were acquired using a mass-to-charge (m/z) range of 50–1350 with a scan time of 0.5 s.

2.5. SFC-PDA-MS conditions

SFC separations were performed on a 4.6 mm × 150 mm, 3 µm Chiralpak IC (Chiral Technologies, West Chester, PA, USA) by gradient elution at a flow rate of 3.0 mL/min and an ABPR pressure of 150 Bar, with the use of a MeOH make-up flow at 1 mL/min. The eluents were CO_2 for solvent A and EtOH for solvent B. The mobile phase gradient was programmed as follows: isocratic hold at 5% B for 2 min, 5 to 30% B from 2 to 18 min, 30 to 50% B from 18 to 30 min and 2 min equilibration time. The column was maintained at a temperature of 40 °C for all analyses. The SFC–PDA–MS settings were as follows: 260 nm PDA detection, positive and negative were acquired using ESI with a capillary voltage of 3.0 kV, cone voltage 30 V, desolvation gas (N2) flow rate 800 L/h, cone gas (N2) flow rate 50 L/h, desolvation temperature at 400 °C and a source temperature 150 °C. Full-scan mass spectra were acquired in the mass-to-charge (m/z) range 100–1500 with a scan time of 0.15 s.

3. Results and discussion

Common sources of process impurities include starting materials and intermediates, byproducts, reagents, catalysts, ligands, residual solvent related impurities, degradation products, and chiral impurities, among others. This study is focused on fate and purge of impurities in 1-uridine, the GMP or regulatory starting material (RSM) used for the synthesis of one of the intermediates (bis-piv 2′ketouridine) related to an anti-HCV therapeutic [51]. A growing trend in the pharmaceutical industry is the preparation of a "background package" when seeking scientific advice from an agency prior to the commercial filing application. Both the FDA (U.S. Food & Drug Administration) and EMA (European Medicines Agency) allow filing a request for scientific advice which includes advice on the acceptability of the GMP starting materials selected for the forthcoming NDA (new drug application) and MAA

(marketing application authorization). The background package for scientific advice contains the detailed chemical characterization of RSMs, particularly ones of considerable complexity such as 1-uridine. In addition, RSMs from different suppliers have to be compared against each other in order to understand all related impurities within these materials across different batches and manufacturing routes. In the case of 1- uridine, the fate and purge of cytidine and ribosyl uridine (two specified impurities found across several 1-uridine batches), had to be investigated in order to establish their control strategy.

Impurity fate mapping is one of the frequently performed studies in the pharmaceutical industry requiring cross-functional collaboration between process chemistry, chemical engineers and analytical chemists toward impurity separation, identification and mapping. Fig. 1 illustrates the 1-uridine oxidation reaction in question subdivided by three steps (protection, isomerization and oxidation), as well as the general strategy for impurity fate and purge that our team followed during this investigation. The first experiment (Fig. 1b) is to understand the downstream fate and potential byproduct formation from each impurity by running the reaction with a molar equivalent of the target impurity in the absence of the SM, 1-uridine. The second step (Fig. 1c) is to spike certain levels of each impurity into the reaction along with the 1-uridine RSM. The subsequent downstream reaction mixture would contain the residual RSMs, desired product, typical process impurities, and in this case, cytidine and ribosyl uridine derivatives. EOR samples in addition to the final isolated dry cake are investigated in detail to see whether the impurities are purged (dry cake – final desired product) and in order to establish the mass balance recovery of the impurity fate during the process workup (EOR and mother liquor: part of a solution that is left over after crystallization), with the preferred outcome being > 70% recovery.

Impurity fate and purge experiments typically require the use of multiple chromatographic methods including RPLC and LC-MS in order to track impurity peaks and their identities between the various methods employed. In this regard, the separation method can become the bottleneck in tracking all the species across the EORs and final isolated dry cakes. The chromatograms overlaid in Fig. 2a were obtained from RPLC-UV analysis of multiple mixtures containing some of the components that are part of this chemistry. The target intermediate bis-piv 2′ketouridine is in equilibrium with the enol form under aqueous conditions, resulting in a very poor chromatographic performance by RPLC (see HPLC trace highlighted in red). In addition, RPLC using a conventional C18 column is unable to retain some impurities formed in the reaction including uracil and 5-bromouracil. Some RPLC stationary phases such as Waters T3 and Hypersil Gold aQ are designed to work under highly hydrophilic conditions and can help to improve retention of very polar compounds known as “fast flyers”, but they don't address the unacceptable on-column keto-enol tautomerization, which in any case, requires extensive mobile phase pH investigation during chromatographic method development.

On the contrary, SFC does not traditionally use water in the mobile phase modifier, in addition to being a great tool for separating polar species. Some key components of this reaction including RSM, desired product and related impurities were subjected to method development screening using both achiral and chiral SFC conditions [14,20,52].

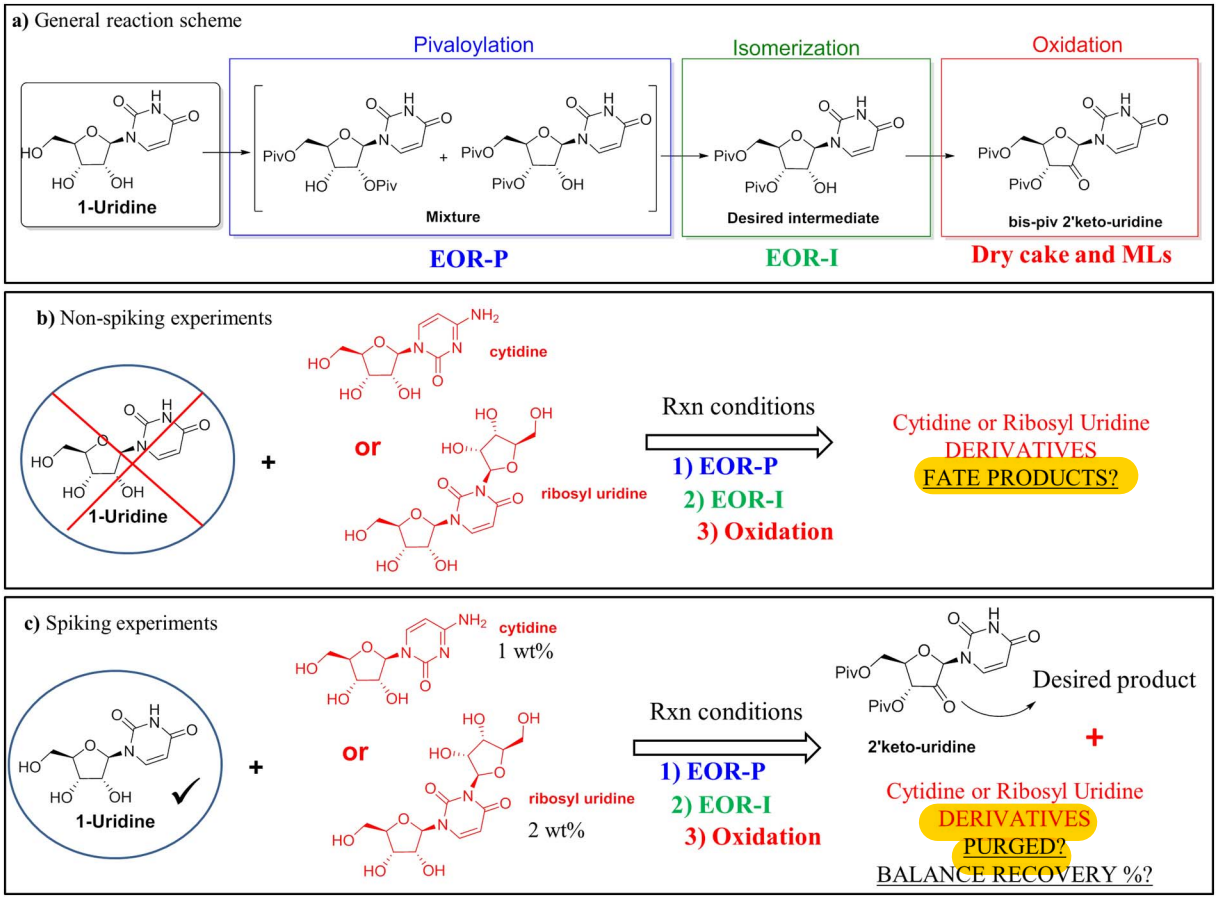

Fig. 1. General strategy steps for investigation of “impurity fate and purge”. a) General reaction scheme for multistep oxidation of 1-uridine to produce the desired 2′keto-uridine intermediate. b) Non-spiking experiments: The impurity itself is used as the starting material. c) Spiking experiments: Certain level of each impurity is spiked into the reaction using 1-uridine starting material. 2% w/w of ribosyl uridine (corresponding to 1.2 LC Area%) and 1% w/w of cytidine (corresponding to 1.18 LC Area%) were spiked into the reaction separately.

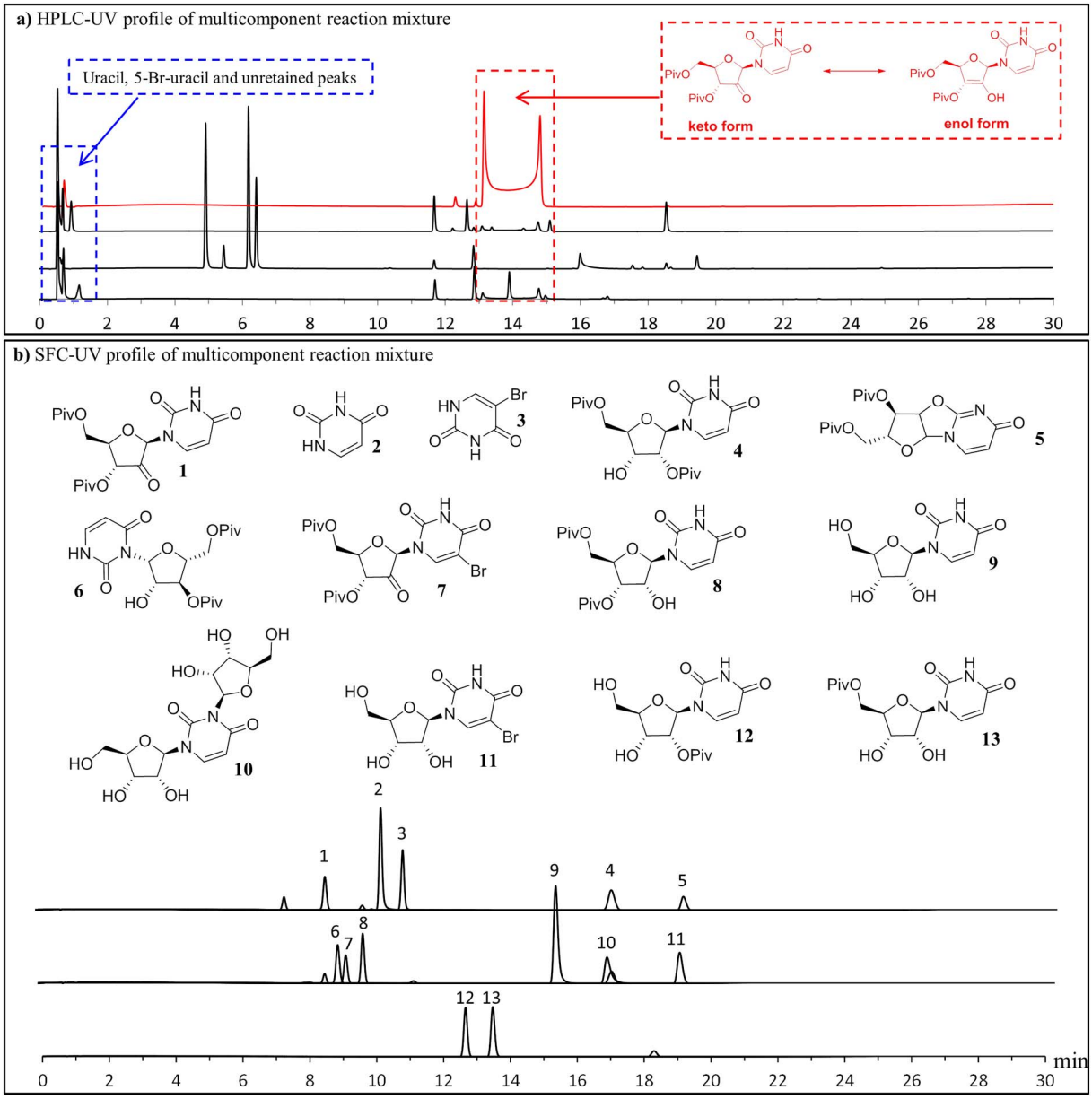

Fig. 2. HPLC *vs* SFC for separation of multicomponent mixtures of 1-uridine oxidation reaction. a) HPLC-UV profile. b) SFC-UV profile. All details on chromatographic method conditions are described in the experimental section. Components 1–13 illustrated in this figure: bis-piv 2′ketouridine (1), uracil (2), 5-bromouracil (3), Bis-Piv Uridine (3′-OH) (4), bis-piv uridine cyclic impurity (5), bis-piv uridine *N*-isomer (6), 5-bromo bis-piv2′ketouridine (7), bis-piv uridine (2′-OH) (8), uridine (9), ribosyl uridine (10), 5-bromouridine (11), mono-piv uridine (3′5′OH) (12), 5-bromouracil (3), mono-Piv Uridine (2′3′OH) (13). Three chromatographic traces related to three different mixtures are presented in order to avoid potential reactions and stability issues.

Interestingly, SFC-UV analysis (Fig. 2b) using a polysaccharide-based chiral selector bonded to 3 µm fully porous particles (Chiralpak IC, 4.6 × 150 mm column) delivers excellent peak shape and retention for all components (1 − 13). The use of chiral columns for achiral separations is a very effective approach that has been extensively applied to the analysis of closely related species [13,26,48] and multicomponent reaction mixtures [45]. In many of these cases, the use of a chiral stationary phase along with SFC delivers substantially better performance compared to an achiral phase with SFC or RPLC [13]. SFC conditions for this method include the use of an EtOH/CO_2 based mobile phase eluent which allows for direct MS detection with the use of a MeOH make-up flow at 1 mL/min.

SFC combined with tandem UV and MS detectors is quickly becoming an excellent tool to enable direct reaction monitoring [45]. In this particular scenario, the separation power of the SFC method using a chiral column combined with UV and MS detection serves to get peak area% while simultaneously providing mass data of each component in a single experimental run. Fate and purge of ribosyl uridine and cytidine derivatives across multiple EOR samples, mother liquors (MLs) and final isolated dry cake was determined by extensive SFC-PDA-MS analysis. Tables 1 and 2 consolidate the data for all reaction components including the desired product and other related impurities. All of the corresponding structures are shown in Fig. 3. Fate derivatives from both impurities are highlighted for a better visualization of the impurity fate mapping and balance recovery (%). In general, because the structure of ribosyl uridine and cytosine are closely related to 1-uridine, it is expected that they follow a similar reaction pattern; with pivaloyalated species after EOR-P, isomerization after EOR-I and oxidized derivatives mostly rejected in the MLs. It is important to point out that by the time that fate and purge experiments are carried out, most of the byproduct

Table 1
Ribosyl uridine spiking experiments.

		Area%*				MS data		
No	t_R (min)	EOR-P	EOR-I	Dry cake	MLs	MW	ESI-MS prominent ions $[M + H]^+$ (m/z)	ESI-MS prominent ions $[M-H]^-$ (m/z)
1	5.37		0.15			712.79	713.4, 735.4 (M + Na)	
2	5.94	0.3				712.79	713.4, 735.4 (M + Na)	
3	6.34				0.41	410.42	411.3	409.2
4	6.5	0.21	0.15			712.79	713.4, 735.4 (M + Na)	
5	6.74		0.14			712.79	713.4, 735.4 (M + Na)	
6	6.77				0.54	489.32	490.15	488.15
7	7.13	0.31				712.79	713.4, 735.4 (M + Na)	
8	7.52	0.22				712.79	713.4, 735.4 (M + Na)	
9	7.95		0.27			712.79	713.4, 735.4 (M + Na)	
10	8.31	4.74	5	0.26	3.84	496.56	497.1, 519.2 (M + Na)	495.4
11	8.46			99.74	5.1	410.42	411.2	409.2
12	8.86		0.32			412.44	435.2 (M + Na)	411.3
13	9.52	54.62	88.03			412.44	413.4, 435.2 (M + Na)	411.2
14	10.17				42.3	112.03		110.98
15	10.79				41.3	190.98	190.9	188.9
16	11.67				1.81	428.44	429.2, 451.2 (M + Na)	
17	16.82	39.6	4.36			412.44	413.2, 435.2 (M + Na)	411.2, 823.2 (2 M–H)$^-$
18	19.03		1.56		5.08	394.42	395.2	393.2

* Recovery of the ribosyl uridine spike = (area% of fate products/area% of ribosyl uridine spike) × 100 = 0.95/1.2 * 100 = 79%.

Table 2
Cytidine spiking experiments.

		Area%*				MS data		
No	t_R (min)	EOR-P	EOR-I	Dry cake	MLs	MW	ESI-MS prominent ions $[M + H]^+$ (m/z)	ESI-MS prominent ions $[M-H]^-$ (m/z)
19	4.92	0.07	0.06		0.17	579.69	580.3, 385.2, 196.0	578.3
20	6.27	0.53	0.65			495.57	496.3, 301.3, 196.0	494.3, 410.2194.1
21	6.71				1.05	511.57	512.2, 494.2	
22	7.93	0.35	0.23			495.57	496.3, 301.1, 196.1	494.4, 410.4, 194.2
10	8.3	5.2	5.13	0.27	16.63	496.56	497.1, 519.1 (M + Na)	495.3, 409.4, 366.2
11	8.46			99.73	28.83	410.42	411.2	409.2
23	9.09				6.25	489.32	489.2	487.1
13	9.51	52.62	91.02			412.44	413.3	411.3
14	10.17				13.17	112.09		110.98
15	10.79				33.37	189.94		188.9
16	11.67				0.53	428.44	429.2, 451.2 (M + Na)	427.18, 409.2
17	16.92	41.23	2.92			412.44	413.1	411.3

* Recovery of the cytidine spike = (area % of fate products/area% of cytidine spike) × 100 = 1.22/1.18 * 100 = 103%.

structures from 1-uridine starting material are already isolated and elucidated. Having these impurities in hand to be used as retention time markers, with a good understanding of their structures and mass spectra, is vital in order to focus the analytical efforts on the impurity fate products.

The ribosyl uridine impurity and its fate in the downstream chemistry are outlined in Table 1 and Fig. 3 (highlighted in red). A fate and purge experiment where 2% *w*/w of ribosyl uridine (corresponding to 1.2 area%), was spiked into the pivaloylation/BF_3 treatment and oxidation steps. The experimental data showed that all products generated from ribosyl uridine were rejected during the chemical workup to non-detectable level (≤0.02 A%), with the desired bis-2'piv ketouridine intermediate isolated in high purity (Dry cake sample: > 99.0%). As a result, this investigation demonstrates that controlling the ribosyl uridine impurity in the 1-uridine starting material at a maximum 0.5 area %, which ensures this impurity is well rejected in the downstream steps and will always meet the any other impurity specification of 0.10 area% in the final API. Note that the area% of the fate products rejected in the MLs is 0.95%, which accounts for about 79% recovery of the ribosyl uridine spike (1.2 area%).

The fate of cytidine in the downstream chemistry is illustrated in Table 2 and Fig. 3 (highlighted in blue). In this case, the fate and purge experiment was performed by spiking 1% w/w of cytidine (corresponding to 1.18 area%) into the reaction using the same reaction conditions as described for the ribosyl uridine experiments. The results showed that all products generated from cytidine are also well-rejected to non-detectable level (≤0.02 A%) and that the desired bis-piv ketouridine intermediate was isolated in high purity (Dry cake sample: > 99.0%). This investigation demonstrates that controlling the cytidine impurity in the 1-uridine starting material at a maximum 0.50 area%, will ensure this impurity is well rejected in the downstream steps and will always meet the impurity specification of 0.10% in the final API. Note that the area% of the fate products in the ML is 1.22%, which accounts for about 103% recovery of the cytidine spike (1.18 area%).

As stated previously, there are no specific regulatory requirements for demonstrating successful impurity fate and purge analysis with respect to identity, mass balance and/or percent recovery of spiked impurities and their downstream analogues. Therefore, the intent of this study was to develop a framework for establishing an acceptable

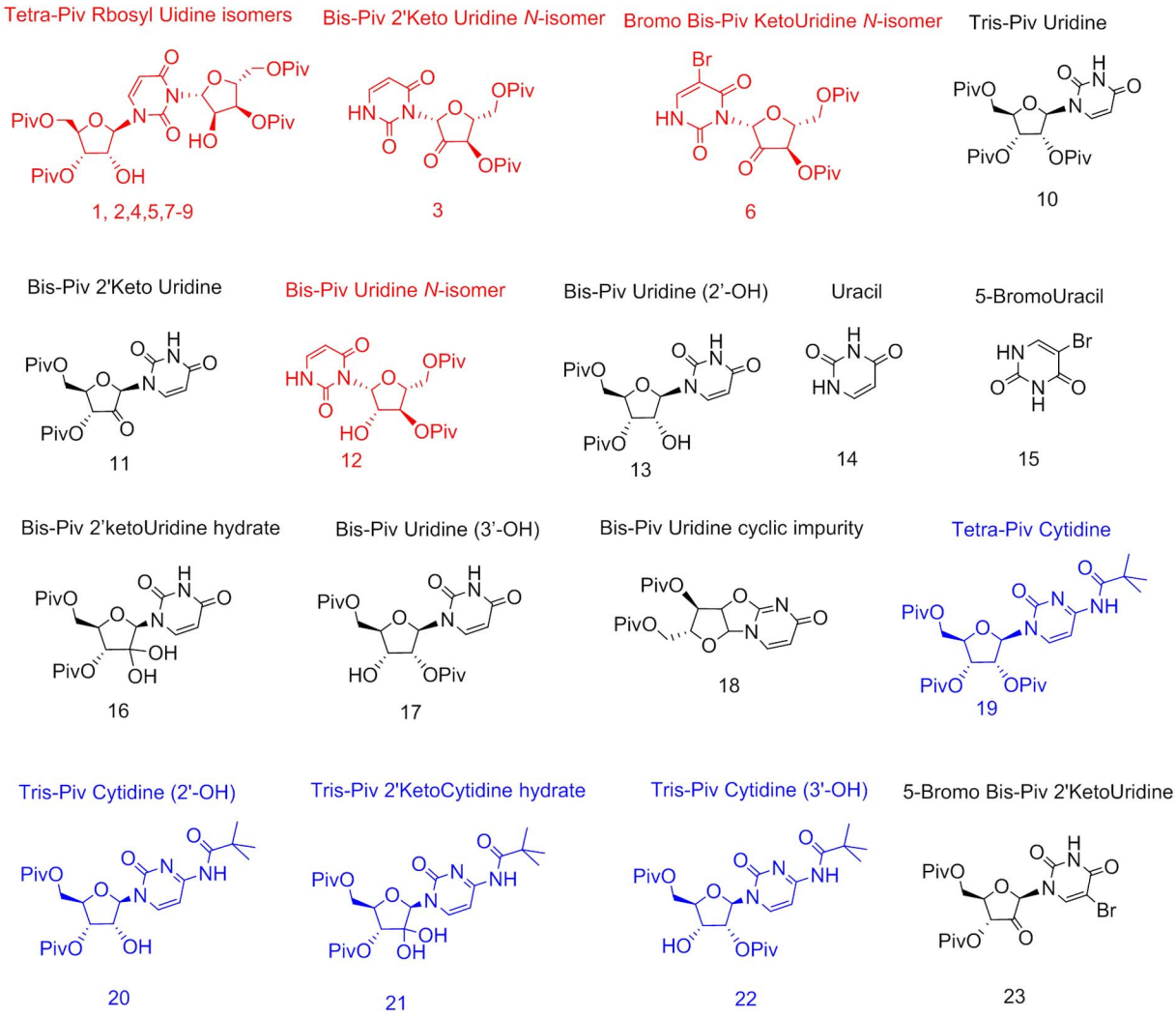

Fig. 3. Structures of all reaction components from ribosyl uridine and cytidine spiking experiments. Compound numbers follow the same order as outlined in Tables 1 and 2. Fate products from spiked impurities are highlighted in red and blue, respectively. (For interpretation of the references to color in this figure legend, the reader is referred to the web version of this article.)

experimental design for sound fate and purge analysis which can be presented in the commercial filing application. This framework serves to establish the mechanism of formation and purge of each impurity and ensure that the fate and purge are well understood. This is vital to ensure that none of the fate products are missing due to peak coelution or poor chromatographic performance. Fig. 4 summarizes the fate mechanism of both impurities investigated in this study.

Briefly, ribosyl uridine (Fig. 4a) is extensively pivaloyalated across both ribose rings as indicated by SFC-MS data showing multiple peaks at m/z = 713 ($[M + H]^+$). New tetra-piv isomers are formed after treatment with boron trifluoride diethyl etherate (BF_3), in addition to a new derivative identified as the bis-piv uridine *N*-isomer based on its molecular ion $[M + Na]^+$ at m/z = 435 and NMR confirmation. These species are rejected during final oxidation in the MLs as bis-piv ketouridine *N*-isomer and its brominated derivative ($[M + H]^+$ at m/z = 411 and 490, respectively). On the other hand, cytidine (Fig. 4b) produces tris and tetra-piv cytidine isomers during pivaloylation followed by BF_3 treatment as indicated by SFC-MS analysis ($[M + H]^+$ at m/z = 496 and 580, respectively). Tris-piv ketocytidine hydrate ($[M + H]^+$ at m/z = 512) is formed during the oxidation step, and together with tetra-piv cytidine, is rejected in the MLs workup.

4. Conclusions

In this study the use of SFC-PDA-MS for fate and purge of impurities in pharmaceutical process research and development was investigated in order to establish an effective impurity control strategy for 1-uridine, the starting material used for the synthesis of the bis-piv 2'keto-uridine intermediate related to an anti-HCV therapeutic. Readily available SFC instrumentation with a chiral column (Chiralpak IC) and EtOH:CO_2 based mobile phase eluent enabled the separation of closely related components from complex reaction mixtures where RLPC failed to deliver optimal chromatographic performance. The combination of SFC with PDA and ESI-MS detection allowed for direct ribosyl uridine and cytidine fate mapping across multiple reaction steps. These results along with the systematic process and recovery requirements establish a framework for appropriate fate and purge experimentation for commercial filing application of a new drug substance. Additionally, the results of this study suggest that existing SFC-PDA-MS instrumentation can be expanded to new applications into the research and development of new medicines.

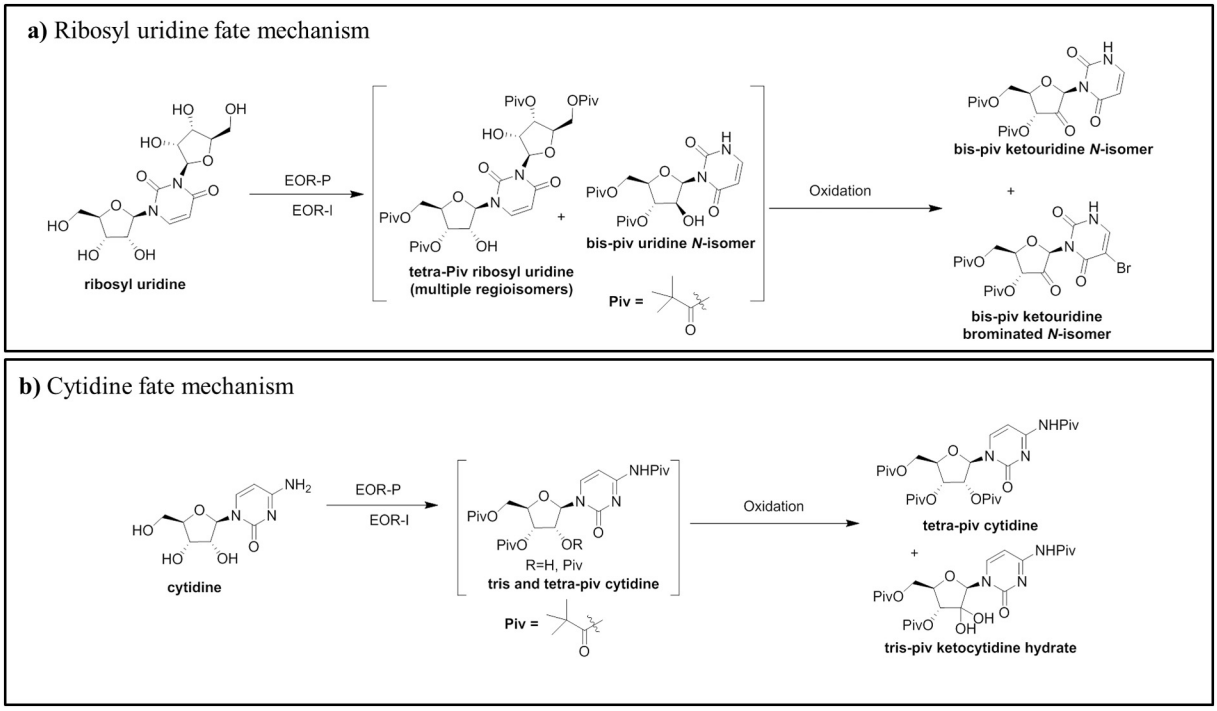

Fig. 4. Proposed pathways and structures for the fate and purge of ribosyl uridine (a) and cytidine (b) impurities in 1-uridine starting material.

Acknowledgements

We thank Mr. Ryan Cohen for helping on the NMR analysis and structure elucidation of some of the impurities presented here. We also thank Dr. Justin R. Denton for valuable discussions on the chromatography of these reaction mixtures.

References

[1] G. Szekely, M.C. Amores de Sousa, M. Gil, F. Castelo Ferreira, W. Heggie, Genotoxic impurities in pharmaceutical manufacturing: sources, regulations, and mitigation, Chem. Rev. 115 (2015) 8182–8229.
[2] U. Yadav, P. Dhiman, N. Malik, A. Khatkar, N. Redhu, D.P. Singh, Genotoxic impurities - an overview, J. Biomed. Pharm. Res. 2 (2013) 39–47.
[3] N.K. Lapanja, R.T. Casar, S. Jurca, B. Doljak, Theoretical purge factor determination as a control strategy for potential mutagenic impurities in the synthesis of drug substances, Acta Chim. Slov. 64 (2017) 1–14.
[4] A. Teasdale, D. Elder, S.-J. Chang, S. Wang, R. Thompson, N. Benz, I.H. Sanchez Flores, Risk assessment of Genotoxic impurities in new chemical entities: strategies to demonstrate control, Org. Process. Res. Dev. 17 (2013) 221–230.
[5] L.-C. Campeau, Q. Chen, D. Gauvreau, M. Girardin, K. Belyk, P. Maligres, G. Zhou, C. Gu, W. Zhang, L. Tan, P.D. O'Shea, A robust kilo-scale synthesis of Doravirine, Org. Process. Res. Dev. 20 (2016) 1476–1481.
[6] Y. Li, D.Q. Liu, S. Yang, R. Sudini, M.A. McGuire, D.S. Bhanushali, A.S. Kord, Analytical control of process impurities in Pazopanib hydrochloride by impurity fate mapping, J. Pharm. Biomed. Anal. 52 (2010) 493–507.
[7] A.V.B. Reddy, J. Jaafar, K. Umar, Z.A. Majid, A.B. Aris, J. Talib, G. Madhavi, Identification, control strategies, and analytical approaches for the determination of potential genotoxic impurities in pharmaceuticals: a comprehensive review, J. Sep. Sci. 38 (2015) 764–779.
[8] D.Q. Liu, A.S. Kord, Analytical challenges in stability testing for genotoxic impurities, Trends Anal. Chem. 49 (2013) 108–117.
[9] D. Jain, P.K. Basniwal, Forced degradation and impurity profiling: recent trends in analytical perspectives, J. Pharm. Biomed. Anal. 86 (2013) 11–35.
[10] C.L. Barhate, E.L. Regalado, N.D. Contrella, J. Lee, J. Jo, A.A. Makarov, D.W. Armstrong, C.J. Welch, Ultrafast chiral chromatography as the second dimension in two-dimensional liquid chromatography experiments, Anal. Chem. 89 (2017) 3545–3553.
[11] D.R. Stoll, P.W. Carr, Two-dimensional liquid chromatography: a state of the art tutorial, Anal. Chem. (2016), http://dx.doi.org/10.1021/acs.analchem.6b03506.
[12] B.W.J. Pirok, A.F.G. Gargano, P.J. Schoenmakers, Optimizing separations in on-line comprehensive two-dimensional liquid chromatography, J. Sep. Sci. (2017) 1–30, http://dx.doi.org/10.1002/jssc.201700863.
[13] E.L. Regalado, C.J. Welch, Separation of achiral analytes using supercritical fluid chromatography with chiral stationary phases, Trends Anal. Chem. 67 (2015) 74–81.
[14] E.L. Regalado, P. Zhuang, Y. Chen, A.A. Makarov, N. McGachy, C.J. Welch, Chromatographic resolution of closely related species in pharmaceutical chemistry: dehalogenation impurities and mixtures of halogen isomers, Anal. Chem. 86 (2014) 805–813.
[15] E.L. Regalado, W. Schafer, R. McClain, C.J. Welch, Chromatographic resolution of closely related species: separation of warfarin and hydroxylated isomers, J. Chromatogr. A 1314 (2013) 266–275.
[16] E.L. Regalado, R. Helmy, M.D. Green, C.J. Welch, Chromatographic resolution of closely related species: drug metabolites and analogs, J. Sep. Sci. 37 (2014) 1094–1102.
[17] F.T. Mattrey, A.A. Makarov, E.L. Regalado, F. Bernardoni, M. Figus, M.B. Hicks, J. Zheng, L. Wang, W. Schafer, V. Antonucci, S.E. Hamilton, K. Zawatzky, C.J. Welch, Current challenges and future prospects in chromatographic method development for pharmaceutical research, TrAC Trends Anal. Chem. 95 (2017) 36–46.
[18] D. Guillarme, M.W. Dong, Newer developments in HPLC impacting pharmaceutical analysis: a brief review, Am. Pharm. Rev. 16 (2013) 38–43.
[19] A. Makarov, R. LoBrutto, Y. Kazakevich, Liophilic mobile phase additives in reversed phase HPLC, J. Liq. Chromatogr. Relat. Technol. 31 (2008) 1533–1567.
[20] C.L. Barhate, L.A. Joyce, A.A. Makarov, K. Zawatzky, F. Bernardoni, W.A. Schafer, D.W. Armstrong, C.J. Welch, E.L. Regalado, Ultrafast chiral separations for high throughput enantiopurity analysis, Chem. Commun. 53 (2017) 509–512.
[21] E. Lesellier, C. West, The many faces of packed column supercritical fluid chromatography: a critical review, J. Chromatogr. A 1382 (2015) 2–46.
[22] M.B. Hicks, E.L. Regalado, F. Tan, X. Gong, C.J. Welch, Supercritical fluid chromatography for GMP analysis in support of pharmaceutical development and manufacturing activities, J. Pharm. Biomed. Anal. 117 (2016) 316–324.
[23] L. Miller, Use of dichloromethane for preparative supercritical fluid chromatographic enantioseparations, J. Chromatogr. A 1363 (2014) 323–330.
[24] C.J. Venkatramani, M. Al-Sayah, G. Li, M. Goel, J. Girotti, L. Zang, L. Wigman, P. Yehl, N. Chetwyn, Simultaneous achiral-chiral analysis of pharmaceutical compounds using two-dimensional reversed phase liquid chromatography-supercritical fluid chromatography, Talanta 148 (2016) 548–555.
[25] E.L. Regalado, C.J. Welch, Pushing the speed limit in enantioselective supercritical fluid chromatography, J. Sep. Sci. 38 (2015) 2826–2832.
[26] T. Shibata, S. Shinkura, A. Ohnishi, K. Ueda, Achiral molecular recognition of aromatic position isomers by polysaccharide-based CSPs in relation to chiral recognition, Molecules 22 (2017) 38.
[27] A. Dispas, V. Desfontaine, B. Andri, P. Lebrun, D. Kotoni, A. Clarke, D. Guillarme, P. Hubert, Quantitative determination of salbutamol sulfate impurities using achiral supercritical fluid chromatography, J. Pharm. Biomed. Anal. 134 (2017) 170–180.
[28] C.M. Galea, Y. Vander Heyden, D. Mangelings, Chapter 12 - separation of stereoisomers, in: C.F. Poole (Ed.), Supercritical Fluid Chromatography, Elsevier, 2017, pp. 345–379.
[29] T.A. Berger, B.K. Berger, Minimizing UV noise in supercritical fluid chromatography. I. Improving back pressure regulator pressure noise, J. Chromatogr. A 1218 (2011) 2320–2326.
[30] R. Helmy, M. Biba, J. Zang, B. Mao, K. Fogelman, V. Vlachos, P. Hosek, C.J. Welch, Improving sensitivity in chiral supercritical fluid chromatography for analysis of

active pharmaceutical ingredients, Chirality 19 (2007) 787–792.
[31] T.A. Berger, The past, present, and future of analytical supercritical fluid chromatography, Chromatographia Today, 2014, pp. 26–29.
[32] V. Desfontaine, J.L. Veuthey, D. Guillarme, Chapter 8 - hyphenated detectors: mass spectrometry, in: C.F. Poole (Ed.), Supercritical Fluid Chromatography, Elsevier, 2017, pp. 213–244.
[33] A. Grand-Guillaume Perrenoud, J.-L. Veuthey, D. Guillarme, Coupling state-of-the-art supercritical fluid chromatography and mass spectrometry: from hyphenation interface optimization to high-sensitivity analysis of pharmaceutical compounds, J. Chromatogr. A 1339 (2014) 174–184.
[34] K. Zawatzky, M. Biba, E.L. Regalado, C.J. Welch, MISER chiral supercritical fluid chromatography for high throughput analysis of enantiopurity, J. Chromatogr. A 1429 (2016) 374–379.
[35] E. Lemasson, S. Bertin, P. Hennig, E. Lesellier, C. West, Comparison of ultra-high performance methods in liquid and supercritical fluid chromatography coupled to electrospray ionization-mass spectrometry for impurity profiling of drug candidates, J. Chromatogr. A 1472 (2017) 117–128.
[36] D. Spaggiari, F. Mehl, V. Desfontaine, A. Grand-Guillaume Perrenoud, S. Fekete, S. Rudaz, D. Guillarme, Comparison of liquid chromatography and supercritical fluid chromatography coupled to compact single quadrupole mass spectrometer for targeted in vitro metabolism assay, J. Chromatogr. A 1371 (2014) 244–256.
[37] K. Takahashi, S. Kinugasa, M. Senda, K. Kimizuka, K. Fukushima, T. Matsumoto, Y. Shibata, J. Christensen, Quantitative comparison of a corona-charged aerosol detector and an evaporative light-scattering detector for the analysis of a synthetic polymer by supercritical fluid chromatography, J. Chromatogr. A 1193 (2008) 151–155.
[38] M. Lecoeur, N. Simon, V.r. Sautou, B. Decaudin, C. Vaccher, A chemometric approach to elucidate the parameter impact in the hyphenation of evaporative light scattering detector to supercritical fluid chromatography, J. Chromatogr. A 1333 (2014) 124–133.
[39] E. Lesellier, A. Valarché, C. West, M. Dreux, Effects of selected parameters on the response of the evaporative light scattering detector in supercritical fluid chromatography, J. Chromatogr. A 1250 (2012) 220–226.
[40] X. Bu, E.L. Regalado, J. Cuff, W. Schafer, X. Gong, Chiral analysis of poor UV absorbing pharmaceuticals by supercritical fluid chromatography-charged aerosol detection, J. Supercrit. Fluids 116 (2016) 20–25.
[41] L. Nováková, A. Grand-Guillaume Perrenoud, I. Francois, C. West, E. Lesellier, D. Guillarme, Modern analytical supercritical fluid chromatography using columns packed with sub-μm particles: a tutorial, Anal. Chim. Acta 824 (2014) 18–35.
[42] C.L. Barhate, M.F. Wahaba, Z.S. Breitbach, D.S. Bell, D.W. Armstrong, High efficiency, narrow particle size distribution, sub-2 μm based macrocyclic glycopeptide chiral stationary phases in HPLC and SFC, Anal. Chim. Acta 898 (2015) 128–137.
[43] C. West, E. Lemasson, S. Bertin, P. Hennig, E. Lesellier, An improved classification of stationary phases for ultra-high performance supercritical fluid chromatography, J. Chromatogr. A 1440 (2016) 212–228.
[44] L. Nováková, V. Desfontaine, F. Ponzetto, R. Nicoli, M. Saugy, J.-L. Veuthey, D. Guillarme, Fast and sensitive supercritical fluid chromatography - tandem mass spectrometry multi-class screening method for the determination of doping agents in urine, Anal. Chim. Acta 915 (2016) 102–110.
[45] E.L. Regalado, M.C. Kozlowski, J. Curto, T. Ritter, M.G. Campbell, A.R. Mazzotti, B. Hamper, C.D. Spilling, M.P. Mannino, L. Wan, J.-Q. Yu, J. Liu, C.J. Welch, Support of academic synthetic chemistry using advanced separation technologies from the pharmaceutical industry, Org. Biomol. Chem. 12 (2014) 2161–2166.
[46] J.M. Płotka, M. Biziuk, C. Morrison, J. Namieśnik, Pharmaceutical and forensic drug applications of chiral supercritical fluid chromatography, Trends Anal. Chem. 56 (2014) 74–89.
[47] L.A. Joyce, E.L. Regalado, C.J. Welch, Hydroxypyridyl imines: enhancing chromatographic separation and stereochemical analysis of chiral amines via circular dichroism, J. Organomet. Chem. 81 (2016) 8199–8205.
[48] H. Xin, Z. Dai, J. Cai, Y. Ke, H. Shi, Q. Fu, Y. Jin, X. Liang, Rapid purification of diastereoisomers from piper kadsura using supercritical fluid chromatography with chiral stationary phases, J. Chromatogr. A 1509 (2017) 141–146.
[49] C. West, J. Melin, H. Ansouri, M.l. Mengue Metogo, Unravelling the effects of mobile phase additives in supercritical fluid chromatography. Part I: polarity and acidity of the mobile phase, J. Chromatogr. A 1492 (2017) 136–143.
[50] D.-R. Wu, S.H. Yip, P. Li, D. Sun, J. Kempson, A. Mathur, Additive free preparative chiral SFC separations of 2,2-dimethyl-3-aryl-propanoic acids, J. Pharm. Biomed. Anal. 131 (2016) 54–63.
[51] H. Wedemeyer, D. Wyles, R. Reddy, A. Luetkemeyer, I. Jacobson, J.M. Vierling, S. Gordon, R. Nahass, S. Zeuzem, J. Wahl, E. Barr, B.Y.T. Nguyen, M. Robertson, H.K. Joeng, H. Liu, P. Jumes, F. Dutko, E. Martin, Safety and efficacy of the fixed-dose combination regimen of MK-3682/grazoprevir/ruzasvir in cirrhotic or non-cirrhotic patients with chronic HCV GT1 infection who previously failed a direct-acting antiviral regimen (C-SURGE), J. Hepatol. 66 (2017) S85.
[52] W. Schafer, T. Chandresekaran, Z. Pirzada, C. Zhang, X. Gong, M. Biba, E.L. Regalado, C.J. Welch, Improved chiral SFC screening for analytical method development, Chirality 25 (2013) 799–804.